ARTICLE IN PRESS

Earth and Planetary Science Letters ∎ (∎∎∎∎) ∎∎∎–∎∎∎

Contents lists available at SciVerse ScienceDirect

Earth and Planetary Science Letters

journal homepage: www.elsevier.com/locate/epsl

# Seismic structure of the Central US crust and shallow upper mantle: Uniqueness of the Reelfoot Rift

Fred F. Pollitz*, Walter D. Mooney

*USGS, 345 Middlefield Road, MS 977, Menlo Park, CA 94025, USA*

ARTICLE INFO

*Article history:*
Accepted 21 May 2013
Editor: P. Shearer

*Keywords:*
seismic surface waves
mantle
New Madrid Seismic Zone

ABSTRACT

Using seismic surface waves recorded with Earthscope's Transportable Array, we apply surface wave imaging to determine 3D seismic velocity in the crust and uppermost mantle. Our images span several Proterozoic and early Cambrian rift zones (Mid-Continent Rift, Rough Creek Graben—Rome trough, Birmingham trough, Southern Oklahoma Aulacogen, and Reelfoot Rift). While ancient rifts are generally associated with low crustal velocity because of the presence of thick sedimentary sequences, the Reelfoot Rift is unique in its association with low mantle seismic velocity. Its mantle low-velocity zone (LVZ) is exceptionally pronounced and extends down to at least 200 km depth. This LVZ is of variable width, being relatively narrow (~50 km wide) within the northern Reelfoot Rift, which hosts the New Madrid Seismic Zone (NMSZ). We hypothesize that this mantle volume is weaker than its surroundings and that the Reelfoot Rift consequently has relatively low elastic plate thickness, which would tend to concentrate tectonic stress within this zone. No other intraplate ancient rift zone is known to be associated with such a deep mantle low-velocity anomaly, which suggests that the NMSZ is more susceptible to external stress perturbations than other ancient rift zones.

Published by Elsevier B.V.

## 1. Introduction

Three $M$~7–8 events in the New Madrid Seismic Zone in 1811–1812 are among the largest historical earthquakes in the United States (NMSZ) (Johnston, 1996; Hough, 2008). Studies of large paleoliquefaction features indicate that there were at least two sequences of large earthquakes in about 1450 and 900 A.D. that look like repeats of the 1811–1812 sequence (Tuttle et al., 2002). Additional studies reveal a history of large earthquakes in the Holocene at several other localities around the margins of the NMSZ (e.g. Harrison et al., 1999; Al-Shukri et al., 2005). The NMSZ is a 300-km-long and narrow zone of predominantly strike–slip faulting within the Reelfoot Rift, a reactivated Precambrian rift zone (Fig. 1). These large and rare intraplate events are enigmatic because the lack of pervasive crustal deformation suggests that the NMSZ has been active for a geologically relatively short time (Schweig and Ellis, 1994), contemporary strain rates are small compared to the rate of Holocene activity (Newman et al., 1999; Calais et al., 2010; Frankel et al., 2012), and the mechanism of stress concentration is unresolved (Grana and Richardson, 1996; Stuart et al., 1997; Liu and Zoback, 1997; Kenner and Segall, 2000; Grollimund and Zoback, 2001; Pollitz et al., 2001; Mazzotti, 2007).

Focal mechanism studies and other stress indicators indicate that intraplate–earthquakes in the central and eastern US, including the SSW-NNE-trending NMSZ, are consistent with an ENE-WSW compressive stress field that acts on pre-existing faults (Sbar and Sykes, 1973; Zoback and Zoback, 1980; Braile et al., 1982; Zoback and Zoback, 1989). The existence of pre-existing faults in the NMSZ provides a zone of weakness but does not indicate how the faults are loaded. A lower crustal detachment fault has been proposed to concentrate crustal stress (Stuart et al., 1997), though such a fault has not been corroborated by seismic data. A mechanical strength contrast between the Reelfoot rift and the Missouri batholith can localize stress in the zone of their intersection (Long, 1976; Campbell, 1978; Hildenbrand, 1985), but this mechanism still requires a recent increase in strain rate arising from external factors.

Geophysical models to explain the initiation and repeated occurrence of large seismic events in the NMSZ have focussed on the origin of Holocene and late Pleistocene stress perturbations and crustal heterogeneities. A weak (i.e. low-viscosity) lower crust can focus stresses on the overlying crust (Liu and Zoback, 1997; Kenner and Segall, 2000; Pollitz et al., 2001), but there is no independent evidence that such a low-viscosity zone exists. Exceptional models that invoke mantle weakness are the models of Grollimund and Zoback (2001) and Forte et al. (2007), which invoke a pre-existing weak mantle to generate flow fields likely connected with the crustal stress field—driven by either glacio-isostatic adjustment or Farallon slab sinking, respectively.

* Corresponding author. Tel.: +1 6503294821; fax: +1 6503295143.
*E-mail addresses:* fpollitz@usgs.gov (F.F. Pollitz), mooney@usgs.gov (W.D. Mooney).

0012-821X/$ - see front matter Published by Elsevier B.V.
http://dx.doi.org/10.1016/j.epsl.2013.05.042

Please cite this article as: Pollitz, F.F., Mooney, W.D., Seismic structure of the Central US crust and shallow upper mantle: Uniqueness of the Reelfoot Rift. Earth and Planetary Science Letters (2013), http://dx.doi.org/10.1016/j.epsl.2013.05.042

ARTICLE IN PRESS



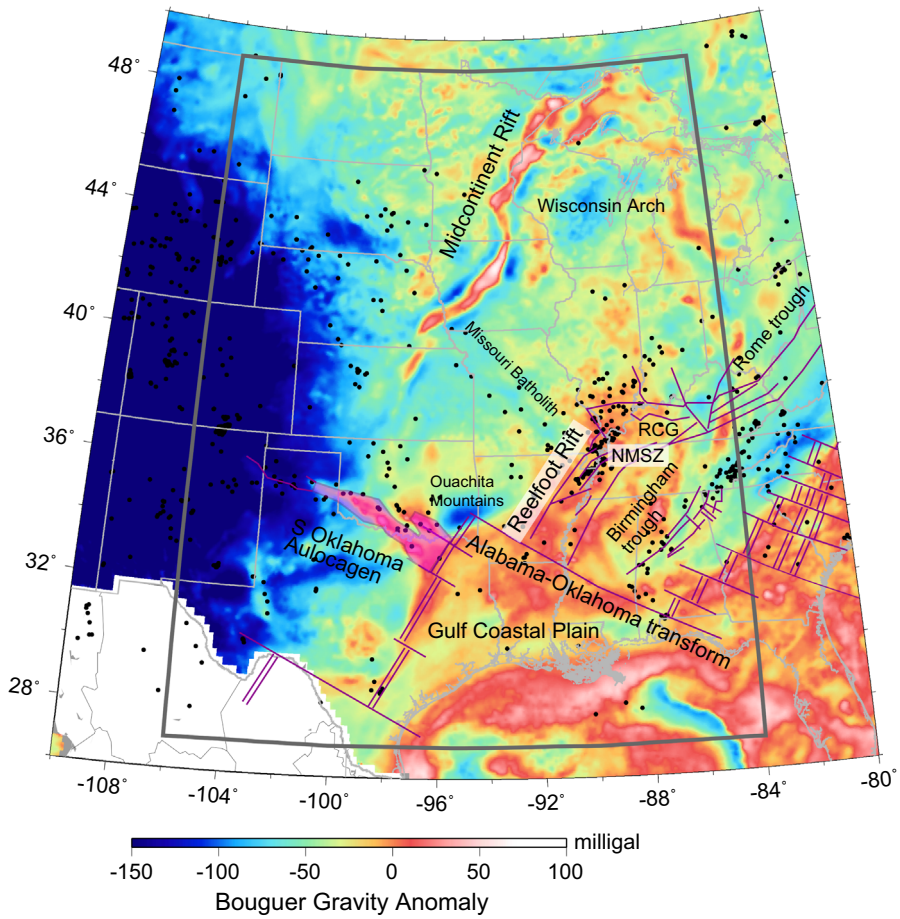


**Fig. 1.** Bouguer gravity map of the central United States with lines of inferred basement faults superimposed following Thomas (2006). Gravity data was obtained from the National Geophysical Data Center at: http://www.ngdc.noaa.gov/. Small black circles are epicenters of $M \geq 3.0$ events of depth ≤50 km from 1978 to 2008 obtained from the National Earthquake Information Center (NEIC) catalog at http://earthquake.usgs.gov/eqcenter/. RCG, Rough Creek Graben; NMSZ, New Madrid Seismic Zone.

The notion of a weak mantle is disputed by McKenna et al. (2007) on the basis of the lack of evidence for a thermal anomaly.

The Central and Eastern United States (CEUS) is a mosaic of several Proterozoic igneous and volcanic provinces subjected to repeated episodes of continental collision and rifting (Thomas, 2006; Whitmeyer and Karlstrom, 2007). The CEUS contains several Proterozoic and early Cambrian rift zones (Fig. 1) with associated crustal extension, igneous intrusion and volcanism (Van Arsdale, 2009a; Thomas, 2010). The Reelfoot Rift is one of the ancient rift zones and was formed in early Paleozoic (Van Arsdale and Cox, 2007). Geophysical investigations of the Reelfoot Rift and NMSZ have revealed fragmentary details of the crust and underlying mantle structure. A high-velocity seismic anomaly within the deep crust below the NMSZ has been inferred with seismic and magnetotelluric data (Mooney et al., 1983; Hildenbrand and Hendricks, 1995) and interpreted as a remnant of basaltic intrusion. Local and regional body wave tomography suggests that the mantle beneath the Reelfoot Rift is of relatively low velocity (Bedle and van der Lee, 2006; Zhang et al., 2009). The crustal structure has been placed into a regional context using ambient noise tomography using Rayleigh waves at periods up to 15 s by Liang and Langston (2008), who found good correlations of crustal seismic velocity with ancient rift structures.

In this study we use seismic data from Earthscope's Transportable Array (TA) to estimate Rayleigh wave phase velocity structure at periods up to 125 s, permitting the estimation of 3D perturbations in seismic shear-wave velocity in the uppermost mantle of the Central US. This provides new constraints on the deep structure of all ancient rifts and yields a new perspective on the possible relationship of mantle structure with ancient inherited crustal structures throughout the Central US. We believe that this is key to understanding what distinguishes the Reelfoot Rift from other ancient rifts and the mechanism of stress concentration at the NMSZ.

## 2. Surface-wave imaging

We employ the non-plane surface-wave imaging method of Pollitz and Snoke (2010), which uses fits of Rayleigh wave spectra to determine local phase velocity at fixed periods. The overall strategy of the method is described in the Appendix. The surface wave data set is updated from Pollitz and Snoke (2010), using 125,326 seismograms recording seismic waves generated by 305 teleseismic events of magnitude ≥6.3 and depth ≤75 km which occurred through early September 2012. Complex amplitude spectra of fundamental-mode Rayleigh waves are obtained at selected periods by means of a three-step process. First, for each vertical component seismogram, a spectrogram is constructed using a moving-window taper designed for the period being considered. Second, complex amplitude spectra are obtained at the group-velocity peaks corresponding to the fundamental mode. Third, quality criteria are applied based on the consistency of the group-velocity peaks as a function of period, resulting in a large edited dataset. At a fixed period and spatial location, a grid search is used to fit the complex amplitude spectra in terms of a multi-plane wave fit at trial phase velocities, resulting in an optimal phase local phase velocity (i.e. that associated with minimum

Please cite this article as: Pollitz, F.F., Mooney, W.D., Seismic structure of the Central US crust and shallow upper mantle: Uniqueness of the Reelfoot Rift. Earth and Planetary Science Letters (2013), http://dx.doi.org/10.1016/j.epsl.2013.05.042

misfit); this process is repeated throughout the study area to obtain a continuous map of phase velocity. The phase velocities used in this study are measured at 13 periods (125, 100, 83, 67, 59, 50, 40, 33, 27, 25, 22, 20, and 18 s).

The formal resolution of the phase velocity maps determined with this method is difficult to obtain because the method is a form of imaging rather than tomography (Pollitz and Snoke, 2010). The imaging of phase velocity structure involves neither an inversion nor a forward model, and thus a resolution test involving trial structures (e.g. checkerboard test) is not straightforward. This limitation is shared by the related eikonal tomography method (Lin et al., 2009). (The resolution in our non-plane-wave or the Lin et al. (2009) imaging method could be addressed, in principle, with a large set of numerically determined synthetic seismograms on a laterally heterogeneous earth with fine-scale structure, which could then be put through the imaging procedures of the respective methods.) The length scale of local averaging prescribed by Pollitz and Snoke (2010, Eq. (12)) is of the same order as the ~70 km spacing between the TA instruments, so we regard this as the horizontal resolution of our imaging. The procedure may be judged by the number of rays which pass through sets of TA stations. This is shown in Fig. 2, which shows the direct raypaths from all teleseismic sources (after editing) to all TA stations which provided useful data from recordings of 50-s-period surface waves generated by those sources. The figure illustrates that density of ray coverage is densest in the western part of the study area, where the TA has resided the longest, but is still large in the eastern part of the study area. Numerous raypaths pass through any set of 7 TA stations in the study area (Fig. 2), approximately the number of TA stations that effectively contribute to a local phase velocity determination (Pollitz and Snoke, 2010, Section 3), ensuring a robust determination of local wavenumber and hence phase velocity.

The sensitivity of the shortest period spans the crust and peaks at 25 km depth, and the longest period has a broad sensitivity kernel roughly centered on 180 km. 3D structure is derived from the phase velocity maps using the procedure described in Appendix A of Pollitz and Snoke (2010). Using scaling relations between P-wave and S-wave velocity, this results in the distribution of vertically polarized shear-velocity $v_s$ in the crust and upper mantle. The formal depth range of 3D perturbations is from earth's surface to 240 km depth, somewhat deeper than the depth of maximal sensitivity in order to avoid 'squeezing' of deeper structure into the base of the model domain. The determination of 3D structure uses the Taylor (1989) crustal structure combined with the PREM mantle structure (Dziewonski et al., 1981) as a reference structure (Fig. 3), and it includes a correction for crustal thickness (Fig. 4).

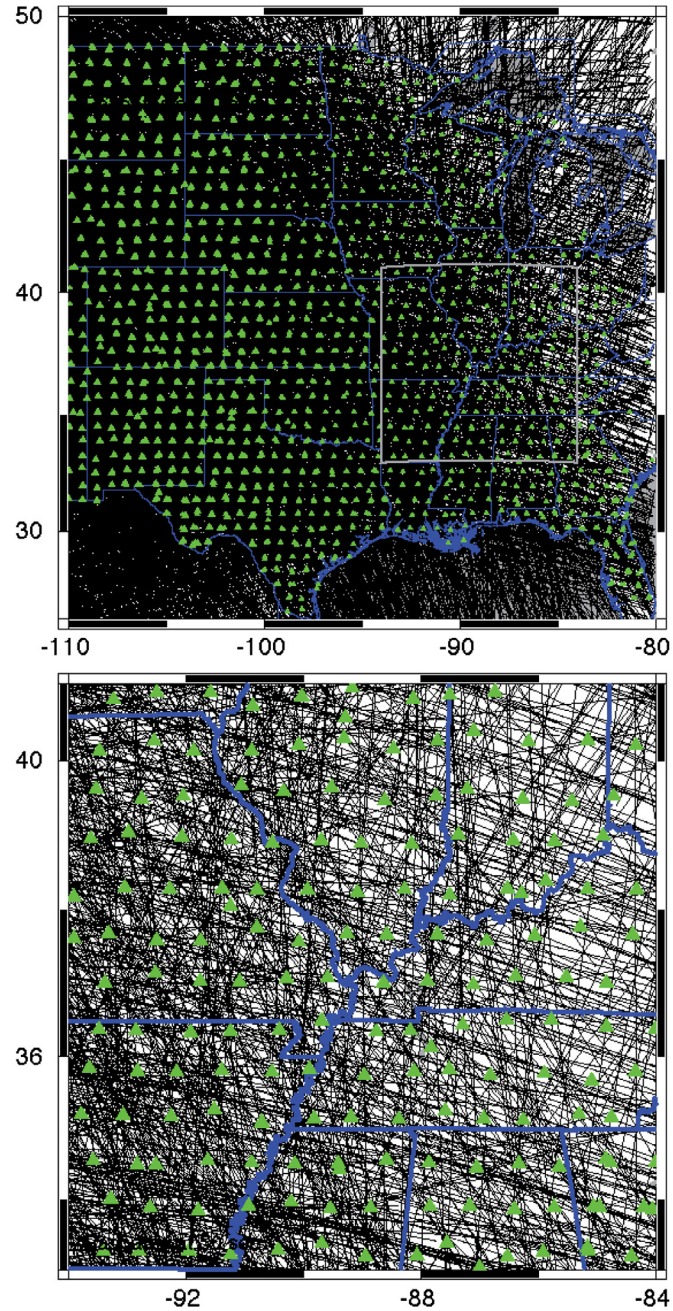


**Fig. 2.** Raypaths between teleseismic sources and TA stations (green triangles) retained after editing at period 50 s. The number of raypaths is subsampled by a factor of 10 in the plots. Bottom plot is a closer view of the Mississippi Embayment region from the upper plot. State boundaries within the United States are shown in blue. (For interpretation of the references to color in this figure legend, the reader is referred to the web version of this article.)

## 3. Results

Rayleigh wave phase velocity maps are presented in Fig. 5, and associated errors at selected periods in Fig. 6. The shorter period maps (i.e. at period ≤27 s) reveal that zones of low phase velocity are correlated with several failed rift zones, i.e. the Mid-Continent Rift, the Rough Creek Graben—Rome trough, the Birmingham trough, and the Southern Oklahoma Aulacogen. The Reelfoot Rift emerges as a coherent low-velocity feature at longer periods ≥50 s. Our phase velocity results are very similar to those obtained independently using Helmholtz tomography (Shen et al., submitted for publication).

Corresponding depth slices of perturbation in logarithmic 3D shear-velocity $v_s$ are shown in Fig. S1. Two of these slices are shown in greater detail in Fig. 7, and alternative perspectives are shown in Fig. S2 in a sequence of regional depth slices and Figs. S3–S6 in volume rendered images. The long linear high-velocity structure stretching from Wisconsin to western Texas at depth ≥65 km may represent depleted mantle associated with the Yavapai and Mazatzal provinces (Whitmeyer and Karlstrom, 2007), and similarly for the high-velocity mantle underlying the area from Indiana to northern Alabama which is part of the Granite-Ryolite Province. All rift structures but the Reelfoot Rift have a shallow expression of the low-velocity zone (LVZ) restricted to depth ≤65 km, whereas the mantle LVZ beneath the Reelfoot Rift extends to depth of at least 200 km (at the limit of the resolving

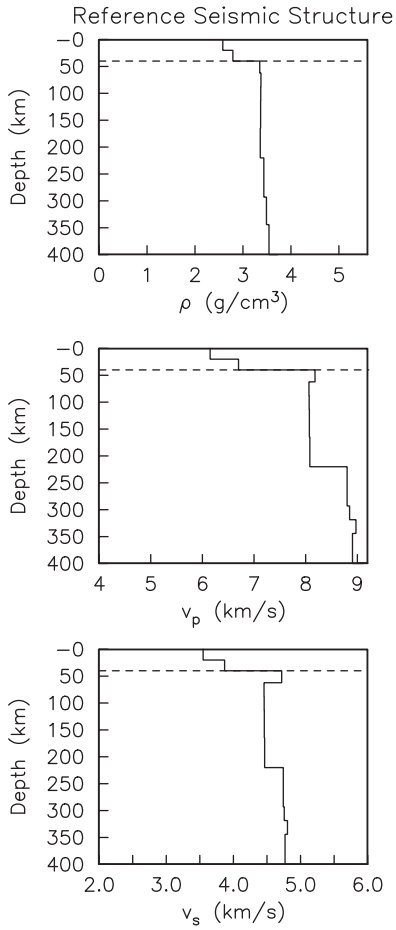


**Fig. 3.** Reference seismic structure of the central US using the crustal structure of Taylor (1989) and mantle structure of PREM (Dziewonski et al., 1981). In the upper 200 km this model is similar to the CR model of the Midwestern US (Chu et al., 2012).

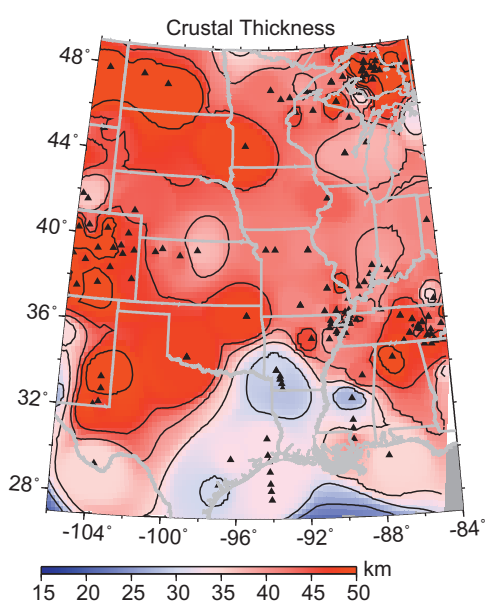


**Fig. 4.** Smoothed crustal thickness over the central-eastern US derived mainly from active-source profiles (Chulick and Mooney, 2002) (with additional subsequent profiles). Contour interval is 5 km. Locations of crustal thickness estimates in that database are indicated with triangles.

power of the surface waves) (Fig. S1). The NMSZ and its principal strike–slip fault (Blytheville fault) lie within a zone of low-velocity mantle, as seen in vertical cross-section AA' in Fig. 8. This pattern of low mantle $v_s$ is consistent with the inferred low-$v_p$ mantle beneath the Reelfoot Rift to at least 160 km depth (Zhang et al., 2009) or deeper (Bedle and van der Lee, 2006).

At its southern end, the Reelfoot Rift is terminated by the Alabama–Oklahoma transform associated with the opening of the Iapetus Ocean (Van Arsdale, 2009a; Thomas, 2010), which is nearly coincident with the structural boundary of the Gulf of Mexico associated with the opening of the Atlantic (Van Arsdale, 2009b). This boundary is seen in our Rayleigh wave imaging (i.e. the 18 s phase velocity map in Fig. 5), similar to boundary seen in Fig. 7f of Liang and Langston (2008). At its northern end, the surface expression of the Reelfoot Rift overlies the narrowest part of the mantle low-velocity zone (Fig. S1).

Seismic velocity in the crust below the NMSZ is relatively fast (profiles AA' and BB' in Fig. 8), in agreement with inferences of a 'rift pillow' within the underlying lower crust (Mooney et al., 1983; Hildenbrand and Hendricks, 1995; Stuart et al., 1997). At long wavelength, our inferred pattern of low crustal velocities to the NW of the NMSZ and high crustal velocities to its SE agrees with the Rayleigh wave phase velocity maps of Liang and Langston (2008); at short wavelength this apparently yields to a different pattern involving relatively high crustal velocity to its west and low crustal velocity to its east (Zhang et al., 2009).

The Chulick and Mooney (2002) crustal thickness map is incomplete over much of the central US. Receiver function studies using the Transportable Array (e.g. Abt et al., 2010; Moidaki et al., 2013) suggest that crustal thickness $T_c$ may differ from the crustal thickness derived from active source seismology (Chulick and Mooney, 2002) by 5 km or greater. For example, small-scale variations of $\pm 5$ km are seen near the Midcontinent Rift (Moidaki et al., 2013) where the Chulick and Mooney (2002) crustal thickness pattern is smooth. We investigate the effect that an error in crustal thickness may have on inferred structure at depth. For this purpose we perform a number of separate inversions for 3D structure, one using a reference value $T_c = 40$ km and others using different values $T_c$ that would represent erroneous departures from a 'true' value of 40 km. The bias introduced by using an erroneous crustal thickness is shown in Fig. 9. Errors up to $\pm 2\%$ in logarithmic shear-velocity may result in the crust, and errors up to 1% may result in the deeper mantle.

Short-period phase velocities have better vertical resolution than long-period phase velocities, i.e. the short-period phase velocities will generally map into a shallower and narrower depth region than long periods because of the shape of the depth-dependent sensitivity kernels (e.g. Pollitz and Snoke, 2010, Fig. S2). Although this can result in the erroneous mapping of crustal structure into structure at depth (e.g. Pollitz, 2008, Fig. 19), this is unlikely the case around the Reelfoot Rift. Short-period (≤25 s) phase velocities are generally high around the Reelfoot Rift (Fig. 5) and are mapped as positive $v_s$ anomalies in the crust (Fig. S1), in contrast with the low phase velocities at longer period and correspondingly low-$v_s$ mantle anomalies (Figs. 7 and S1).

## 4. Discussion

The low-$v_s$ zone beneath the Reelfoot Rift extends to at least ~200 km into the upper mantle (Figs. S1 and 8). All other ancient rift zones in the CEUS, which are thought to represent zones of inherent weakness capable of rupturing in earthquakes, are associated with much less penetrative discontinuities (i.e. restricted to the crust and uppermost mantle).

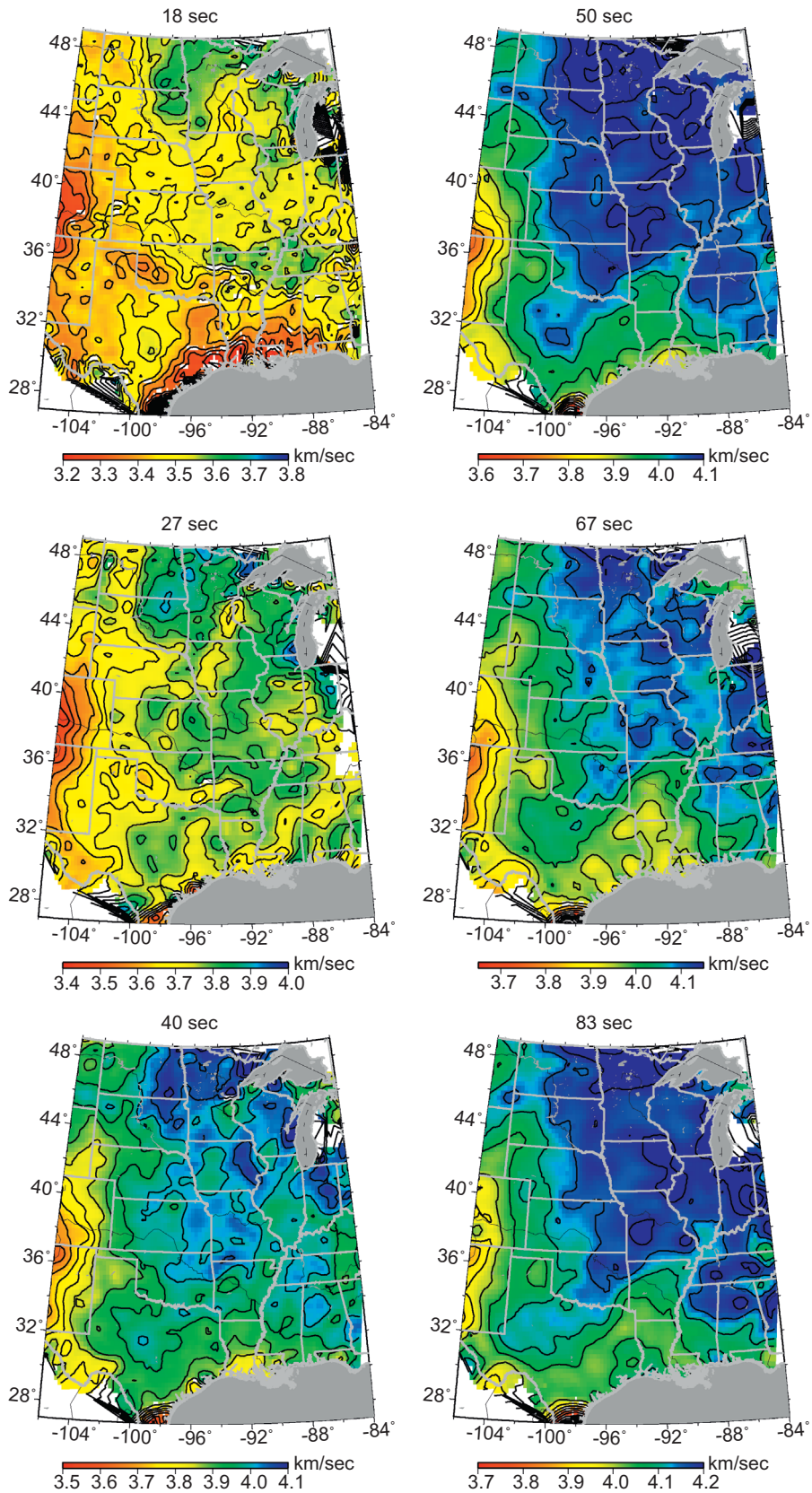


**Fig. 5.** Phase velocity maps of fundamental-mode Rayleigh waves at the indicated periods. Associated standard errors in Fig. 6 tend to be greater at shorter period and greater in the eastern part of the study area because of the data coverage provided by the Transportable Array.

All of the ancient rifts and aulacogens identified in Fig. 1 are associated with positive gravity anomalies to varying degrees, likely because of the presence of shallow basaltic intrusions associated with rifting, as has been documented directly for the Midcontinent Rift (Allen et al., 1992). All are also associated with relatively low crustal seismic velocity (Figs. S1 and 7). Any volumes

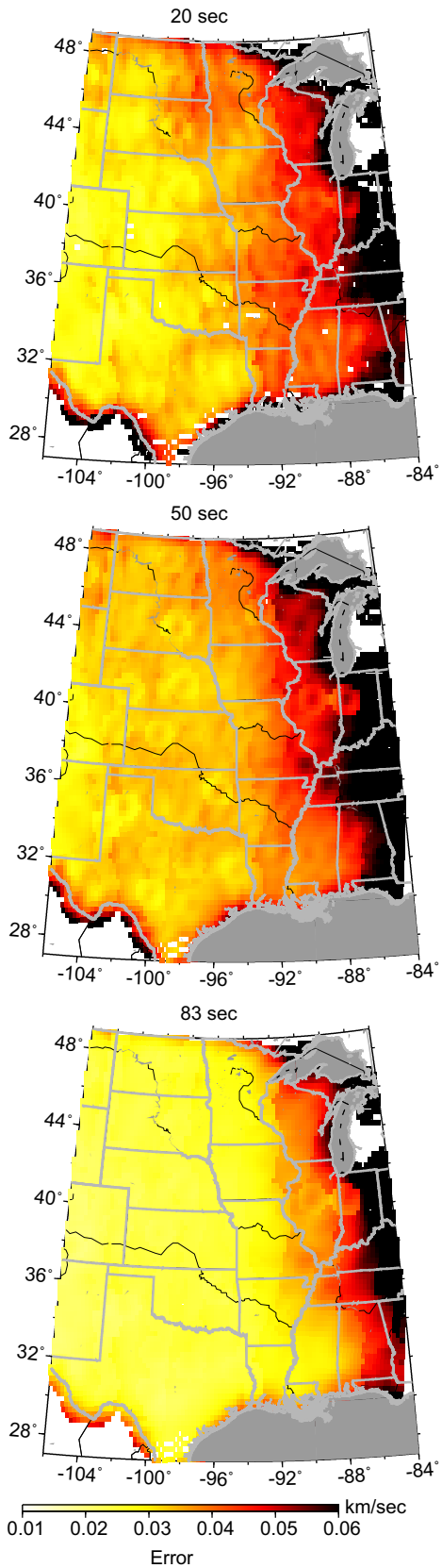


**Fig. 6.** Standard errors in phase-velocity distribution.

of high-velocity basaltic intrusions in these rifts are outweighed by the presence of thick sedimentary sequences on the flanks of the rifts (Liang and Langston, 2008), leading to a net low-velocity signal detected by those surface waves sensitive to predominantly crustal structure (period ≤40 s, Fig. 5).

The Reelfoot Rift formed as part of a series of failed rift basins in the Early-to-Middle Cambrian (520–500 Ma) concurrently with the Rome Trough and Rough Creek Graben to its northeast (Thomas, 2006). These rifts formed within a pre-existing tectonic terrane – the Eastern Ryolite-Granite Province – which was likely continuous over a broad area including the incipient rifts (Whitmeyer and Karlstrom, 2007). The low-$v_s$ signal is most pronounced at depth ≥100 km and varies laterally along the Reelfoot Rift and a northeastern extension that coincides with the Wabash Valley Seismic Zone (WVSZ) (Kim, 2003; Merino et al., 2010), judging from the mantle $v_s$ pattern (Figs. S1 and 7). The mantle low-$v_s$ zone is ~200 km wide zone below the southern Reelfoot Rift, thins to ~50 km around the northern Reelfoot Rift, and widens to ~100 km along the WVSZ. Whether this variable width is a measure of variable extension associated with Cambrian rifting, or it reflects the width of the zone subjected to subsequent modification, is unclear.

The zone of low-$v_s$ mantle extending southwestward from the NMSZ approximately coincides with the Mississippi Embayment (ME), where sediment thickness can be high, raising the possibility that low-velocity sediments could project to great depth as an artifact of the 3D velocity inversion. This is not the case because sediment thickness is not remarkably large in the northern ME compared with surrounding regions (such as the Illinois Basin), according to the sediment thickness map presented in Fig. 4 of Mooney and Kaban (2010). Sediment thickness is relatively large, exceeding 5 km, only in the ME south of Tennessee. This pattern is mimicked in the phase velocity patterns at periods sensitive to crustal structure (≤33 s), which are characterized by relatively high phase velocities in the northern ME and very low phase velocities further south, i.e. south of the fossil Alabama–Oklahoma transform. Low phase velocities beneath the northern ME are realized only at longer periods ≥50 s, which demands a deep source for the corresponding low seismic velocities.

The origin of the low-$v_s$ mantle may be either thermal or compositional. We propose that, as a pre-existing zone of fractured lithosphere, the passage of the Bermuda hotspot beneath the Mississippi Embayment ca. 100 Ma (Van Arsdale and Cox, 2007) led to infiltration of melt in the shallow mantle throughout the NE-SW-trending axis of the embayment. This is consistent with the notion that pre-existing rifted continental lithosphere is more susceptible than surrounding cratonic lithosphere to penetration by magmatism from an impinging plume head (Burov et al., 2007). This led to thermal uplift of the entire Mississippi Embayment (Van Arsdale and Cox, 2007) and may have resulted in compositional changes within the pre-existing weak zone in two ways:

(1) Metasomatism of a mantle peridotite is capable of lowering $v_s$. For example, antigorite, phlogopite, chlorite, and talc are stable at the pressure and temperature conditions of the observed $v_s$ anomaly (Pawley and Wood, 1995; Bose and Ganguly, 1995; Ulmer and Trommsdorff, 1999; Trønnes, 2002; Frost, 2006; Grove et al., 2006), and the presence of these minerals is expected to reduce seismic velocity (Hacker et al., 2005; Mainprice et al., 2008). The hotspot may have provided a source of water to accomplish such mineral transformations. Metasomatic alteration has also been proposed in an Archean subduction zone setting, in order to explain a localized and dipping low-velocity zone within the central Slave craton, Canada (Chen et al., 2009). The alteration envisaged for the Reelfoot Rift alternatively could have taken place during the Alleghanian Orogeny during closure of the Iapetus; a NE-SW trending high-density body along the Grenville–Appalachian suture, proposed to be a remnant slab associated with this

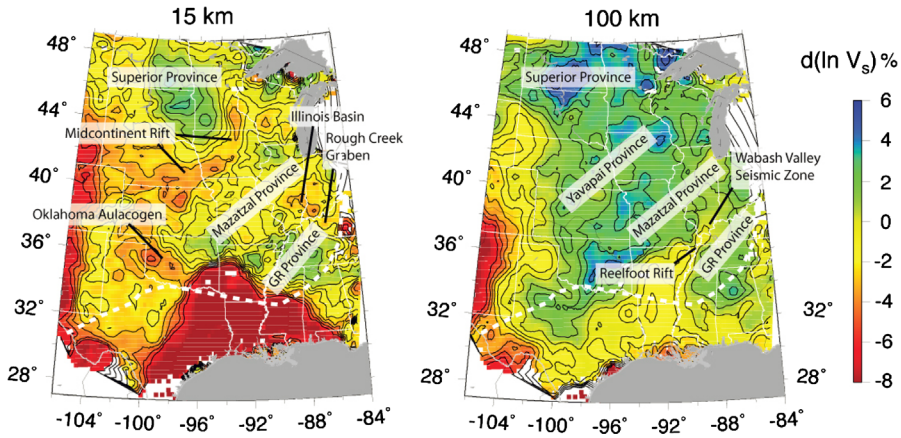


**Fig. 7.** Close-up view of perturbation in $v_s$ with respect to the central US reference model (Fig. 3) in horizontal depth slices at 15 and 100 km depth. Salient features are the shallow expressions of the Midcontinent Rift, Oklahoma Aulacogen, and Rough Creek Graben and the deep expressions of Proterozoic domains (Superior Province, Mazatzal Province, and Granite-Ryolite Province) and the Cambrian Reelfoot Rift. Geologic domains follow Whitmeyer and Karlstrom (2007). Dashed white line is the Grenville front (Thomas, 2006).

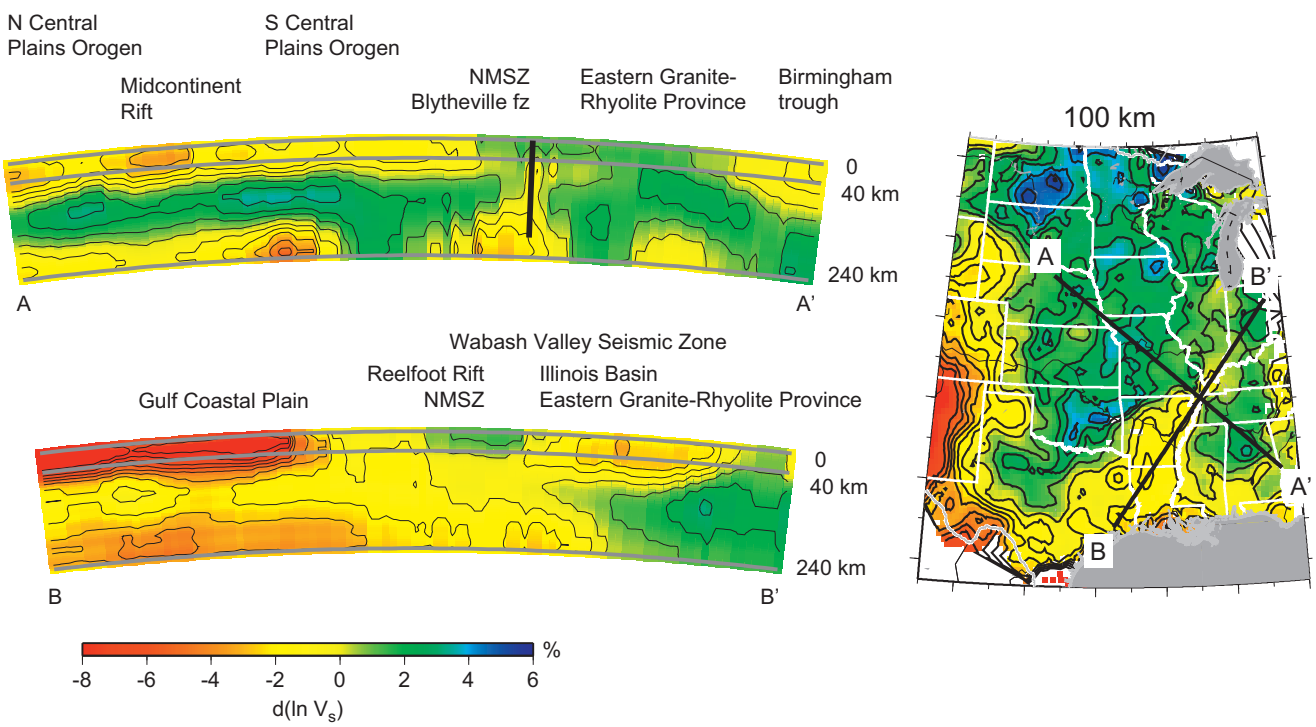


**Fig. 8.** Perturbation in $v_s$ along two vertical cross-sections passing through the NMSZ (locations in inset). Geologic domains follow Van Schmus et al. (1996).

closure (Mooney and Kaban, 2010, Fig. 13, based on the gravity modeling), supports this possibility. In any case, layered phyllosilicates are generally weak and susceptible to sliding in the stable-sliding regime (Peacock and Hyndman, 1999; Moore and Lockner, 2007); if this regime exists in the uppermost mantle beneath the Reelfoot Rift it could provide a mechanism for lowering of its shear strength.

(2) Ascending magma from the hotspot may have emplaced primitive mantle into the mantle below the Reelfoot Rift. Such mantle is relatively dense due to enrichment of Fe relative to the surrounding mantle of the East Granite-Ryolite Province, which is likely depleted, and this compositional difference will also lower $v_s$. This mechanism, involving emplacement of fertile melts in a pre-existing weak zone, has also been proposed by Villemaire et al. (in press) to explain low-velocity mantle beneath the trace of the Great Meteor hotspot beneath southeast Canada, particularly where it intersects the Ottawa-Bonnechere graben, a late Precambrian failed rift zone. A significant residual thermal anomaly is unlikely given the 100 Myr age of the last known heating event. This is supported by the formation of the Mississippi Embayment through subsidence within 30 Myr after passage of the Bermuda hotspot (Van Arsdale and Cox, 2007); further cooling is expected to produce only a low-amplitude and long-wavelength residual thermal anomaly, as indicated by thermal calculations of the temperature anomaly expected ~100 Myr after a hotspot-induced heating event (Eaton and Frederiksen, 2007).

Lateral discontinuities in mantle seismic velocity may signify a discontinuity in shear strength, as suggested above, or a discontinuity

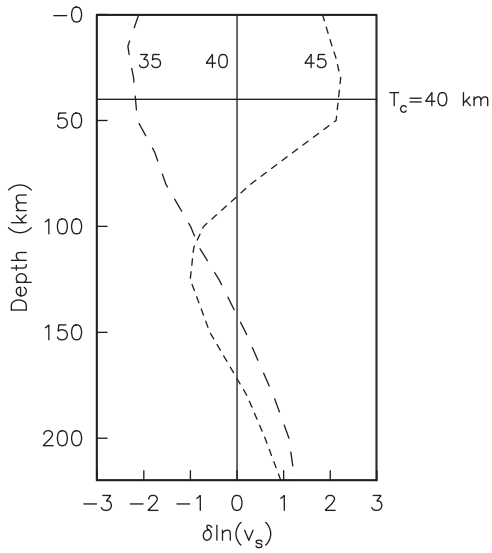


**Fig. 9.** Bias in depth-dependent logarithmic shear-velocity resulting from inverting phase velocity data using crustal thickness $T_c$=35 or 45 km when the 'true' thickness is 40 km. Numerals refer to $T_c$ in km.

in mantle viscosity. In the latter case, models of long-term mantle flow indicate that stress concentration in the crust above such a mantle discontinuity may arise from the discontinuous mantle flow field (Vilotte et al., 1986; Neil and Houseman, 1997; Dayem et al., 2009). Observationally, a mantle strength contrast is often correlated with the presence of a major strike–slip fault in plate boundary zones (e.g. San Andreas fault, North Anatolian fault, Kunlun fault) (Molnar and Dayem, 2010).

The NMSZ can be characterized as overlying a 'trough' in mantle strength, bounded by relatively strong lithosphere to its northwest and southeast—dry and depleted rocks that are part of the Granite-Ryolite Province (Fig. S2). This is similar to the situation of the Laguna Salada and related faults which ruptured in the 2010 M7.2 El Mayor-Cucapah earthquake, Baja California, which is located at a trough in mantle viscosity (Pollitz et al., 2012). Stresses within a shear zone underlain by relatively low-viscosity mantle and surrounded by much stronger lithosphere will scale inversely with the width of the shear zone (Pollitz, 2001). The relatively low elastic plate thickness within the shear zone is an effective mechanism for stress concentration around a strike–slip fault zone provided that the boundaries of the shear zone have some 'long term' relative motion, as is typical at an active plate boundary but questionable at the NMSZ (Calais et al., 2010). Whether the mantle flow field applicable to the NMSZ region is an ambient flow field (as would be typical near an active plate boundary) or a passive flow field in response to a recent forcing event, such as deglaciation, remains an open question.

## 5. Conclusions

Using seismic surface-wave imaging we have constrained the seismic shear-wave velocity structure of the CEUS down to about 240 km depth. Our images confirm the presence of high-velocity cratonic lithosphere in areas interior to rifting and convergence episodes of the Proterozoic and early Phanerozoic periods. They also show that traces of this earlier tectonic activity previously recognized in the regional crustal structure, particularly the development of failed rift zones during the opening of the Iapetus Ocean (Liang and Langston, 2008), are also evident in the regional mantle structure.

Most ancient rift zones in the central US are associated with a seismic signature restricted to the crust and shallow (≲65 km depth) mantle. The Reelfoot Rift low-velocity anomaly extends much deeper. The origin of low-velocity rock beneath the Reelfoot Rift and NMSZ is uncertain but is likely related to a combination of factors that resulted in a compositional seismic-velocity anomaly. This includes magmatism associated with early Cambrian failed rifting, further tectonism at the time of closing of the Iapetus, and magmatism related to passage of the Bermuda hotspot beneath the region ca. 100 Ma (Van Arsdale and Cox, 2007). We hypothesize that past magmatic events altered the composition of the mantle through metasomatic mineral transformations and/or the injection of primitive mantle. In any case, the NMSZ possesses a unique characteristic which sets it apart from other ancient rift zones in North America, and the hypothesized compositional heterogeneity may, through a reduction in shear strength or viscosity in the underlying mantle, reduce the effective elastic plate thickness and consequently concentrate stress in the NMSZ.

Our seismic-velocity results are based on seismic surface-wave imaging with coarse vertical resolution and horizontal resolution ~70 km, i.e. on the order of the spacing between TA instruments. The images provide a sketch of the crust and shallow upper mantle structure that will eventually be complemented by body-wave tomography using the TA as well as higher-resolution images expected to result from regional seismic experiments around the ancient rift zones (e.g. Stein et al., 2011; Marshak et al., 2011; Langston et al., 2011). Images of the mantle velocity structure may also be improved through additional estimates of crustal thickness using the Transportable Array, complementing those based on active-source seismology used here, through receiver-function analysis (e.g. Shen et al., 2013).

## Acknowledgments

Seismic waveform data was obtained from the Incorporated Research Institutions for Seismology (IRIS) Data Management Center. We thank Tom Pratt and Joe Fletcher for internal reviews and John Evans for discussions. We are grateful to Mike Ritzwoller, an anonymous reviewer, and the Editor for their constructive criticisms which helped improve this work.

## Appendix A. Methodology for determining surface-wave phase-velocity maps

Following the methodology of Pollitz and Snoke (2010), phase velocity maps are derived by modelling the surface wavefield recorded by each event as a solution of the 2-D wave equation on a spherical membrane with laterally varying phase velocity. At a given period, this equation is valid in the presence of smooth structural perturbations (Tromp and Dahlen, 1993; Friederich et al., 2000), and it is further applicable to the case of relatively rough lateral variations (those which change on the scale of one propagating wavelength) provided that the seismic network is dense enough to account for the interference of multiple plane waves arriving from different directions (Friederich et al., 2000). In an approach related to 2-plane and multiplane wave tomography (Friederich and Wielandt, 1995; Forsyth et al., 1998; Pollitz, 1999; Forsyth and Li, 2005; Yang and Forsyth, 2006; Yang et al., 2008), following Pollitz and Snoke (2010) we account for interfering plane waves and local phase velocity structure simultaneously by parametrizing each observed wavefield as a weighted sum of the HG (2-D-Hermite–Gaussian) solutions of Friederich and Wielandt (1995), which implicitly depend upon the local phase velocity. Using observations restricted essentially to a subset of USArray

stations about a given locality, we solve simultaneously for the sets of event-HG weighting coefficients plus the local phase velocity using a grid search. This method is simpler than conventional multiplane-wave tomography and, by taking advantage of the large number of events observed by local arrays of stations, results in robust estimates of phase velocity over the entire area spanned by the TA.

The HG-paramterized solution of multiple plane waves approximately satisfies the governing equations of coupled surface waves, i.e. Eqs. (2.28)–(2.30) of Zhou et al. (2004). These equations account for scattering from structure off the source–receiver great circle and account for finite-frequency effects implicitly through the allowance of multiple plane waves arriving from a continuum of backazimuths. In other words, within a small region (that surrounding a small number of USArray stations) the HG solutions completely represent surface waves that would be produced from multiple mode branches scattered from off-great-circle structure.

Attenuative dispersion is not accounted for, i.e. infinite $Q$ is assumed for the reference structure. With an actual $Q$ value of about 200 and a frequency range of a factor of 6 used in this study, this would result in systematic errors of $\pm$~0.15% in phase velocity on the reference structure. This will map into smooth variations in inverted depth-dependent structure of the same magnitude.

The error in local phase velocity is estimated by propagating errors in measured complex amplitude spectra via Eqs. (6) and (7) of Pollitz and Snoke (2010). At a given period and locality, the errors in the complex amplitude spectra are obtained a posteriori by evaluating the residual variance of these spectra after fitting with the HG representation of multiple plane waves. Typical error in phase velocity measurements at all periods is about 0.02–0.05 km/s (e.g. Fig. 6). The lateral resolution is approximately equal to the Gaussian weighting distance used to restrict the observations contributing to phase velocity estimation at a given locality, which is about 50 km (Pollitz and Snoke, 2010, Eq. (12)).

## Appendix B. Supplementary data

Supplementary data associated with this article can be found in the online version at http://dx.doi.org/10.1016/j.epsl.2013.05.042.

## References

Abt, D., Fischer, K.M., French, S.W., Ford, H.A., Yuan, H., Romanowicz, B., 2010. North American lithospheric discontinuity structure imaged by Ps and Sp receiver functions. J. Geophys. Res. 115, B09301, http://dx.doi.org/10.1029/2009JB006914.

Al-Shukri, H.J., Lemmer, R.E., Mahdi, H.H., Connelly, J.B., 2005. Spatial and temporal characteristics of Paleoseismic features in the Southern terminus of the New Madrid Seismic Zone in Eastern Arkansas. Seismol. Res. Lett. 76, 502–511.

Allen, D.J., Hinze, W.J., Cannon, W.F., 1992. Drainage, topographic, and gravity anomalies in the Lake Superior region: evidence for a 1100 Ma mantle plume. Geophys. Res. Lett. 19, 2118–2122.

Bedle, H., van der Lee, S., 2006. Fossil flat-slab subduction beneath the Illinois Basin, USA. Tectonophysics 424, 53–68.

Bose, K., Ganguly, J., 1995. Experimental and theoretical studies of the stabilities of talc, antigorite and phase A at high pressures with applications to subduction processes. Earth Planet. Sci. Lett. 136, 109–121.

Braile, L.W., Keller, G.R., Hinze, W.J., Lidiak, E.G., 1982. An ancient rift complex and its relation to contemporary seismicity in the New Madrid Seismic Zone. Tectonics 1, 225–237.

Burov, E., Guillou-Frottier, L., d'Acremont, E., Le Pourhiet, L., Cloetingh, S., 2007. Plume head–lithosphere interactions near intra-continental plate boundaries. Tectonophysics 434, 15–38.

Calais, E., Freed, A.M., Van Arsdale, R., Stein, S., 2010. Triggering of New Madrid seismicity by late-Pleistocene erosion. Nature 466, 608–612.

Campbell, D.L., 1978. Investigation of the stress-concentration mechanism for intraplate earthquakes. Geophys. Res. Lett. 5, 477–479.

Chen, C.-W., Rondenay, S., Evans, R.L., Snyder, D.B., 2009. Geophysical detection of relict metasomatism from an Archean (3.5 Ga) subduction zone. Science 326, 1089–1091.

Chu, R., Schmandt, B., Helmberger, D.V., 2012. Upper mantle P velocity structure beneath the Midwestern United States derived from triplicated waveforms. Geochem. Geophys. Geosyst. 13, Q0AK04, http://dx.doi.org/10.1029/2011GC003818.

Chulick, G.S., Mooney, W.D., 2002. Seismic structure of the crust and uppermost mantle of North America and adjacent oceanic basins: a synthesis. Bull. Seismol. Soc. Am. 92, 2478–2492.

Dayem, K.E., Houseman, G.A., Molnar, P., 2009. Localization of shear along a lithospheric strength discontinuity: application of a continuous deformation model to the boundary between Tibet and the Tarim Basin. Tectonics 28, TC3002, http://dx.doi.org/10.1029/2008TC002264.

Dziewonski, A.M., Chou, T.-A., Woodhouse, J.H., 1981. Determination of earthquake source parameters from waveform data for studies of global and regional seismicity. J. Geophys. Res. 86, 2825–2852.

Eaton, D., Frederiksen, A., 2007. Seismic evidence for convective-driven motion of the North American plate. Nature 446, 428–431.

Forsyth, D.W., Li, A., 2005. Array-analysis of two-dimensional variations in surface wave phase velocity and azimuthal anisotropy in the presence of multipathing interference. In: Levander, A., Nolet, G. (Eds.), AGU Geophysical Monograph, vol. 187, Washington, DC, pp. 81–98.

Forsyth, D.W., Webb, S.C., Dorman, L.M., Shen, Y., 1998. Phase velocities of Rayleigh waves in the MELT experiment on the East Pacific rise. Science 22, 1235–1238.

Forte, A.M., Mitrovica, J.X., Moucha, R., Simons, N.A., Grand, S.P., 2007. Descent of ancient Farallon slab drives localized mantle flow below the New Madrid Seismic Zone. Geophys. Res. Lett. 34, http://dx.doi.org/10.1029/2006GL027895.

Frankel, A., Smalley, R., Paul, J., 2012. Significant motions between GPS sites in the New Madrid region: implications for seismic hazard. Bull. Seismol. Soc. Am. 102, 479–489.

Friederich, W., Hunzinger, S., Wielandt, E., 2000. A note on the interpretation of seismic surface waves over three-dimensional structures. Geophys. J. Int. 143, 335–339.

Friederich, W., Wielandt, E., 1995. Interpretation of seismic surface waves in regional networks: joint estimation of wavefield geometry and local phase velocity—method and tests. Geophys. J. Int. 120, 731–744.

Frost, D.J., 2006. The stability of hydrous mantle phases. Rev. Mineral. Geochem. 62, 243–271.

Grana, J.P., Richardson, R.M., 1996. Tectonic stress within the New Madrid Seismic Zone. J. Geophys. Res. 101, 5445–5458.

Grollimund, B., Zoback, M.D., 2001. Did deglaciation trigger intraplate seismicity in the New Madrid Seismic Zone? Geology 29, 175–178.

Grove, T.L., Chatterjee, N., Parman, S.W., Medard, E., 2006. The influence of $H_2O$ on mantle wedge melting. Earth Planet. Sci. Lett. 249, 74–89.

Hacker, B., Luffi, P., Lutkov, V., Minaev, V., Ratschbacher, L., Plank, T., Ducea, M., Patino-Douce, A., McWilliams, M., Metcalf, J., 2005. Near-ultrahigh pressure processing of continental crust: Miocene crustal xenoliths from the Pamir. J. Petrol. 46, 1661–1687.

Harrison, R.W., Hoffman, D., Vaughn, J.D., Palmer, J.R., Wiscombe, C.L., McGeehin, J. P., Stephenson, W.J., Odum, J.K., Williams, R.A., Forman, S.L., 1999. An example of neotectonism in a continental interior—Thebes Gap, Midcontinent, United States. Tectonophysics 305, 399–417.

Hildenbrand, T.G., 1985. Rift structure of the northern Mississippi embayment from analysis of gravity and magnetic data. J. Geophys. Res. 90, 12607–12622.

Hildenbrand, T.G., Hendricks, J.D., 1995. Geophysical setting of the Reelfoot Rift and relation between rift structures and the New Madrid Seismic Zone. In: Shedlock, K.M., Johnson, A.C. (Eds.), Investigations of the New Madrid Seismic Zone, vol. 1538-E. U.S. Geological Survey, pp. 1–30.

Hough, S.E., 2008. Large 19th century earthquakes in eastern/central North America. In: Frechet, J., Meghraoui, M., Stucchi, M., Vogt, J. (Eds.), Historical Seismology. Springer, Dordrecht, Netherlands, pp. 351–367.

Johnston, A.C., 1996. Seismic movement assessment of earthquakes in stable continental regions; III, New Madrid 1811–1812, Charleston 1886 and Lisbon 1755. Geophys. J. Int. 126, 314–344.

Kenner, S.J., Segall, P., 2000. A mechanical model for intraplate earthquakes: application to the New Madrid Seismic Zone. Science 289, 2329–2332, http://dx.doi.org/10.1126/science.289.5488.2329.

Kim, W.-Y., 2003. 18 June 2002 Caborn, Indiana earthquake: reactivation of Ancient Rift in the Wabash Valley Seismic Zone?. Bull. Seismol. Soc. Am. 93, 2201–2211.

Langston, C.A., DeShon, H., Horton, S.P., Powell, C.A., Thomas, W.A., Ammon, C.J., Herrmann, R.B., 2011. Scientific problems and lithospheric targets: the northern embayment lithosphere experiment. Geol Soc. Am. Abstr. Prog. 43 (5), 436.

Liang, C., Langston, C.A., 2008. Ambient seismic noise tomography and structure of eastern North America. J. Geophys. Res. 113, B03309, http://dx.doi.org/10.1029/2007JB005350.

Lin, F.C., Ritzwoller, M.H., Snieder, R., 2009. Eikonal tomography: surface wave tomography by phase front tracking across a regional broad-band array. Geophys. J. Int. 177, 1091–1110.

Liu, L., Zoback, M.D., 1997. Lithospheric strength and intraplate seismicity in the New Madrid Seismic Zone. Tectonics 16, 5585–5595, http://dx.doi.org/10.1029/97TC01467.

Long, L.T., 1976. Speculations concerning southeastern earthquakes, mafic intrusions, gravity anomalies, and stress amplification. Earthquake Notes 47, 29–35.

Mainprice, D., Le Page, Y., Rodgers, J., Joanna, P., 2008. *Ab initio* elastic properties of talc from 0 to 12 GPa: interpretation of seismic velocities at mantle pressures and prediction of auxetic behaviour at low pressure. Earth Planet. Sci. Lett. 274, 327–338.

Marshak, S., Pavlis, G.L., Hamburger, M.W., Hersh, G., Larson, T., Shoemaker, K., 2011. The Ozark-Illinois-Kentucky (OIINK) Earthscope Project: characterizing

cratonic-platform lithosphere in North America's Midcontinent. Geol Soc. Am. Abstr. Prog. 43 (5), 363.

Mazzotti, S., 2007. Geodynamic models for earthquake studies in intraplate North America. In: Stein, S., Mazzotti, S. (Eds.), Continental Intraplate Earthquakes: Science, Hazard, and Policy Issues, vol. 425. Geological Society of America, pp. 17–33.

McKenna, J., Stein, S., Stein, C.A., 2007. Is the New Madrid Seismic Zone hotter and weaker than its surroundings? In: Stein, S., Mazzotti, S. (Eds.), Continental Intraplate Earthquakes: Science, Hazard, and Policy Issues, vol. 425. Geological Society of America Special Paper, pp. 167–175.

Merino, M., Stein, S., Liu, M., Okal, E.A., 2010. Comparison of seismicity rates in the New Madrid and Wabash Valley seismic zones. Seismol. Res. Lett. 81 (6), 951–954.

Moidaki, M., Gao, S.S., Liu, K.H., Atekwana, E., 2013. Crustal thickness and Moho sharpness beneath the Midcontinent rift from receiver functions. Res. Geophys. , http://dx.doi.org/10.4081/4538 3:e1.

Molnar, P., Dayem, K.E., 2010. Major intracontinental strike–slip faults and contrasts in lithospheric strength. Geosphere 6, 444–467.

Mooney, W.D., Andrews, M.C., Ginzburg, A., Peters, D.A., Hamilton, R.M., 1983. Crustal structure of the northern Mississippi Embayment and comparison with other continental rift zones. Tectonophysics 94, 327–348.

Mooney, W.D., Kaban, M.K., 2010. The North American upper mantle: density, composition, and evolution. J. Geophys. Res. 115, B12424, http://dx.doi.org/10.1029/2010JB000866.

Moore, D.E., Lockner, D.A., 2007. Comparative deformation behavior of minerals in serpentinized ultramafic rock: application to the slab–mantle interface in subduction zones. Int. Geol. Rev. 49, 401–415.

Neil, E.A., Houseman, G.A., 1997. Geodynamics of the Tarim Basin and the Tian Shan in Central Asia. Tectonics 571, 571–584, http://dx.doi.org/10.1029/97TC01413.

Newman, A., Stein, S., Weber, J., Engeln, J., Mao, A., Dixon, T., 1999. Slow deformation and lower seismic hazard at the New Madrid Seismic Zone. Science 284, 619–621.

Pawley, A.R., Wood, B.J., 1995. The high-pressure stability of talc and 10 Aa phase: potential storage sites for $H_2O$ in subduction zones. Am. Mineral. 80, 998–1003.

Peacock, S.M., Hyndman, 1999. Hydrous minerals in the mantle wedge and the maximum depth of subduction thrust earthquakes. Geophys. Res. Lett. 26, 2517–2520.

Pollitz, F., Bürgmann, R., Thatcher, W., 2012. The M7.2 2010 El Mayor-Cucapah earthquake illuminates rheological mantle heterogeneity. Geochem. Geophys. Geosyst. 13, Q06002, http://dx.doi.org/10.1029/2012GC004139.

Pollitz, F.F., 1999. Regional velocity structure in northern California from inversion of scattered seismic surface waves. J. Geophys. Res. 104, 15043–15072.

Pollitz, F.F., 2001. Viscoelastic shear zone model of a strike–slip earthquake cycle. J. Geophys. Res. 106, 26541–26560.

Pollitz, F.F., 2008. Observations and interpretation of fundamental mode Rayleigh wavefields recorded by the Transportable Array (USArray). J. Geophys. Res. 113, B10311, http://dx.doi.org/10.1029/2007JB005556.

Pollitz, F.F., Kellogg, L., Bürgmann, R., 2001. Sinking mafic body in a reactivated lower crust: a mechanism for stress concentration at the New Madrid Seismic Zone. Bull. Seismol. Soc. Am. 91, 1882–1897.

Pollitz, F.F., Snoke, J.A., 2010. Rayleigh-wave phase-velocity maps and three-dimensional shear-velocity structure of the western US from local non-plane surface-wave tomography. Geophys. J. Int. 180, 1153–1169.

Sbar, M.L., Sykes, L.R., 1973. Contemporary compressive stress and seismicity in eastern North America: an example of intraplate tectonics. Bull. Seismol. Soc. Am. 84, 1861–1882.

Schweig, E.S., Ellis, M.A., 1994. Reconciling short recurrence intervals with minor deformation in the New Madrid Seismic Zone. Science 264, 1308–1311.

Shen, W., Ritzwoller, M.H., Schulte-Pelkum, V., 2013. A 3-D model of the crust and uppermost mantle beneath the central and western US by joint inversion of receiver functions and surface wave dispersion. J. Geophys. Res. , http://dx.doi.org/10.1029/2012JB009602.

Shen, W., Ritzwoller, M.H., Schulte-Pelkum, V., 2013. Crustal and uppermost mantle structure in the central US encompassing the Midcontinental Rift. J. Geophys. Res., submitted for publication.

Stein, S., van der Lee, S., Jurdy, D., Stein, C., Wiens, D., Wysession, M., Revenaugh, J., Frederiksen, A., Darbyshire, F., Bollman, T., Lodewyk, J., Wolin, E., Merino, M., Tekverk, K., 2011. Learning from failure: the SPREE Mid-Continent Rift experiment. GSA Today 21, 5–7.

Stuart, W.D., Hildenbrand, T.G., Simpson, R.W., 1997. Stressing of the New Madrid Seismic Zone by a lower crust detachment fault. J. Geophys. Res. 102, 27623–27633.

Taylor, S., 1989. Geophysical framework of the Appalachians and adjacent Grenville province. In: Geophysical Framework of the Continental United States, vol. 172. Geological Society of America Memoir, pp. 317–348.

Thomas, W.A., 2006. Tectonic inheritance at a continental margin. GSA Today 16, 4–11.

Thomas, W.A., 2010. Interactions between the southern Appalachian-Ouachita orogenic belt and basement faults in the orogenic footwall and foreland. Geol. Soc. Am. Mem. 206, 897–916.

Tromp, J., Dahlen, F.A., 1993. Variational principles for surface wave propagation on a laterally heterogeneous Earth—III: potential representation. Geophys. J. Int. 112, 195–209.

Trønnes, R.G., 2002. Stability range and decomposition of potassic richterite and phlogopite end members at 5–15 GPa. Mineral. Petrol. 74, 129–148.

Tuttle, M., Schweig, E.S., Sims, J.D., Cafferty, R.H., Wolf, L.W., Haynes, M.L., 2002. The earthquake potential of the New Madrid Seismic Zone. Bull. Seismol. Soc. Am. 92, 2080–2089.

Ulmer, P., Trommsdorff, V., 1999. Phase relations of hydrous mantle subducting to 300 km. In: Fei, Y., Bertka, C.M., Mysen, B.O. (Eds.), Mantle petrology: field observations and high pressure experimentation, vol. 6. Geochemical Society Special Publication, pp. 259–281.

Van Arsdale, R., 2009a. Late Proterozoic and Early Cambrian rifting of the southeastern United States. In: Coward, M.P., Dewey, J.F., Hancock, P.L. (Eds.), Adventures Through Deep Time: The Central Mississippi River Valley and Its Earthquakes, vol. 255. Geological Society of America, pp. 29–32.

Van Arsdale, R., 2009b. Pangea rips apart—the formation of the Gulf of Mexico. In: Coward, M.P., Dewey, J.F., Hancock, P.L. (Eds.), Adventures Through Deep Time: The Central Mississippi River Valley and Its Earthquakes, vol. 255. Geological Society of America, pp. 53–63.

Van Arsdale, R., Cox, R., 2007. The Mississippi's curious origins. Nat. Geosci. (January), 33–39.

Van Schmus, W.R., Bickford, M.E., Turek, A., 1996. Proterozoic geology of the east-central Midcontinent basement. In: Basement and Basins of Eastern North America, vol. 308. Geological Society of America, pp. 7–32.

Villemaire, M., Darbyshire, F.A., Bastow, I.D., 2012. P-wave tomography of Eastern North America: evidence for mantle evolution from Archean to Phanerozoic, and modification during subsequent hotspot tectonism. J. Geophys. Res. 117, http://dx.doi.org/10.1029/2012JB009639.

Vilotte, J.P., Madariaga, R., Daignie'res, M., Zienkiewicz, O.C., 1986. Numerical study of continental collision: influence of buoyancy forces and an initial stiff inclusion. Geophys. J. R. Astron. Soc. 84, 279–310.

Whitmeyer, S.J., Karlstrom, K.E., 2007. Tectonic model for the Proterozoic evolution of North America. Geosphere 3, 220–259.

Yang, Y., Forsyth, D.W., 2006. Rayleigh wave phase velocities, small-scale convection, and azimuthal anisotropy beneath southern California. J. Geophys. Res. 111, http://dx.doi.org/10.1029/2005JB004180.

Yang, Y., Ritzwoller, M.H., Lin, F.C., Moschetti, M.P., Shapiro, N.M., 2008. Structure of the crust and uppermost mantle beneath the western United States revealed by ambient noise and earthquake tomography. J. Geophys. Res. 113, B12310, http://dx.doi.org/10.1029/2008JB005833.

Zhang, Q., Sandvol, E., Liu, M., 2009. Lithospheric velocity structure of the New Madrid Seismic Zone: a joint teleseismic and local P tomographic study. Geophys. Res. Lett. 36, L11305, http://dx.doi.org/10.1029/2009GL037687.

Zhou, Y., Dahlen, F.A., Nolet, G., 2004. Three-dimensional sensitivity kernels for surface wave observables. Geophys. J. Int. 158, 142–168.

Zoback, M.L., Zoback, M.D., 1980. State of stress in the conterminous United States. J. Geophys. Res. 85, 6113–6156.

Zoback, M.L., Zoback, M.D., 1989. Tectonic stress field of the continental United States. Geol. Soc. Am. Mem. 172, 523–539.

Please cite this article as: Pollitz, F.F., Mooney, W.D., Seismic structure of the Central US crust and shallow upper mantle: Uniqueness of the Reelfoot Rift. Earth and Planetary Science Letters (2013), http://dx.doi.org/10.1016/j.epsl.2013.05.042